Materials Research. 2014; 17(4): 817-822
DOI: http://dx.doi.org/10.1590/1516-1439.235713

High Sensitivity Ethanol Gas Sensor Based on Sn-doped ZnO Under Visible Light Irradiation at Low Temperature

Peishuo Zhang, Guofeng Pan*, Bingqiang Zhang, Jiali Zhen, Yicai Sun

Institute of Microelectronic, Hebei University of Technology, Tianjin 300130, China

Received: August 21, 2013; Revised: June 24, 2014

Pure ZnO and 5at%, 7at%, 9at% Sn-doped ZnO materials are prepared by the chemical co-precipitation method. They were annealed by furnace at temperature range of 300-700°C in air for 1h. The ZnO materials are characterized by X-ray diffraction (XRD) and scanning electron microscopy (SEM). The results show that the Sn-doped ZnO materials appear rough porous structures. The maximum sensitivity can be achieved by doping the amount of 7 at%. It has much better sensing performance towards ethanol vapor under visible light irradiation. The response and recovery time are ~1s and ~5s, respectively. The mechanism for the improvement in the sensing properties can be explained with the surface adsorption theory and the photoactivation theory.

Keywords: *Sn-doped ZnO, gas sensor, photoactivation, sensing mechanism*

1. Introduction

During the last decades, gas sensors based on metal oxide semiconductors have attracted the attention of environmentalist and many others for detecting harmful and toxic gases efficiently[1]. Among the materials, ZnO is one of the most promising and useful materials for gas sensors. ZnO is an n-type direct band semiconductor having a wide-band gap (3.4 eV), low resistivity and high transparency in the visible range and high light trapping characteristic[2]. However, the sensitivity of the ZnO material is not sufficiently high[3,4].

Because of the high activation energy of reaction with gas molecules, high temperature (300°C-400°C) is applied for the ZnO gas sensor to get higher response[5-7]. However, high temperature not only leads to high power consumption but also ignites the flammable and explosive gases[8]. Moreover, the long-term application at high temperature could result in the growth of the oxide grain that is a main factor responsible for the long-term stability. In recent years, several efforts have been made to improve the sensitivity and lower the operating temperature, for example, different doping elements, varying preparation technology, UV-irradiation and so on. Among them, doping is an important and effective way to improve the gas properties of semiconductors[9].

There are several works that describe the influence of Sn dopant in the ZnO material[10,11]. In particular, the main reason of being chosen of tin as the dopant in ZnO is to enhance the electrical conductivity. When ZnO is doped Sn, Sn^{4+} substitutes Zn^{2+} site in the ZnO crystal structure resulting in two more free electrons to contribute to the electric conduction. Furthermore, Zn can be easily substituted by Sn and does not result in a large lattice distortion due to their almost equal radius (r_{Zn}^{2+}=0.074nm and r_{Sn}^{4+}=0.069nm). Therefore, Sn substituting Zn is a good candidate as an n-type dopant in ZnO[10].

*e-mail: pgf@hebut.edu.cn

In this work, we reported the fabrication of Sn-doped ZnO materials via chemical co-precipitation method and prepared the ethanol gas sensors of thick films. We investigated the effects of Sn doping on the crystal structure and surface morphology. We also discussed the ethanol sensing properties and sensitive mechanism of gas-sensitivity and photo-sensitivity synergistic effect, which had rare been reported before. A close correlation was found between light irradiation and sensitivity based on which an appropriate mechanism underlying this phenomenon was suggested. This discovery is helpful for the commercial application, however, a lower operating temperature still needs further research.

2. Experimental

2.1. *Preparation of ZnO and Sn-doped ZnO materials*

ZnO materials were prepared by the chemical co-precipitation method starting with zinc acetate ($Zn(CH_3COO)_2$, AR) and sodium hydroxide (NaOH, AR). Before the reaction, zinc acetate and sodium hydroxide were dissolved into deionized water respectively. Then the aqueous solution of sodium hydroxide was added dropwise into the zinc acetate solution under continuous stirring, and the pH value of the final solution was controlled as 7. The precipitate was aged for 24 h, then washed and dried at 80°C, followed by sintering at temperature range of 300-700°C in air for 1h, and finally was ground after cooled to room temperature. The same procedures were used to prepare the Sn-doped ZnO using stannic chloride ($SnCl_4$, AR). The different doping content was 5 at%, 7 at% and 9 at% of Sn respectively, which based on the theoretical calculation of optimum doping content[12]. The samples were named as follows: A0,A5,A7,A9, B0,B5,B7,B9,

C0,C5,C7,C9,D0,D5,D7,D9 (A-300°C, B-500°C, C-600°C, D-700°C annealing temperature; 0-0at%, 5-5at%, 7-7at%, 9-9at% doping).

2.2. *Characterization*

The crystal phases of various ZnO samples were characterized by X-ray diffraction (XRD, RIGAKU-D/MAX2500, Japan). XRD patterns were recorded from 10° to 80°(2θ) with a scanning step of 0.02° s^{-1}. The morphology of the samples were observed by a scanning electron microscopy (SEM,HITACHI-S4800, Japan).

2.3. *Preparation of thick film gas sensor*

To fabricate thick film sensors, each sample was added suitable amount of deionized water to each agate mortar, then ground for about 10 min to form a paste, respectively. The dip-coating method was adopted to fabricate the uniform thick films. The film thickness was generally in the 3-5μm range. Figure 1 shows a schematic diagram of a fabricated sensor. The internal diameter of tube is about 0.8mm. The external diameter of tube is about 1.4mm, and the length is about 4mm. A small Ni-Cr alloy coil was placed through the tube as a heater, which provided the operating temperature of the gas sensor. The similar tubes were described in literature[13,14].

2.4. *Gas response testing*

The gas sensing tests are introduced in a gas sensing test system (WS-30A, Henan Hanwei Electronics Co.Ltd, P.R.China).The static volumetric method is used in the gas sensing test. The schematic of the test system was showed in Figure 2. The load resistor (R1) was connected in series with a gas sensor. The circuit voltage (Vc) was 5V, and output voltage (Vout) was the terminal voltage of the load resistor. The operating temperature of a sensor was adjusted through varying the heating voltage (V_h). By monitoring the output voltage, the resistance of the sensor was measured in air and in the test gas. The gas sensitivity of the sensor was defined as S=Rair/Rgas, where Rair and Rgas were the resistance in air and in a test gas, respectively.

The response time was taken as the time required for the variation in conductance to reach 90% of the equilibrium value after the test gas was injected and the recovery time is taken as the time necessary for the sensor to attain a conductance 10% above the original value in air. In our studies, the testing was carried out in an ambient atmosphere at 30% relative humidity. Prior to the start of each test the sensors were preheated 30 min at the testing temperature to allow the thick films to thermally stabilize.

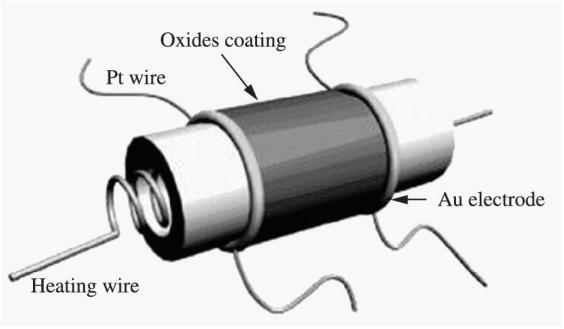

Figure 1. Schematic diagram of the gas sensor structure.

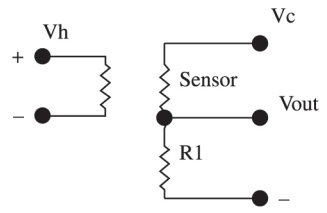

Figure 2. Schematic of the test system.

3. Results and Discussion

3.1. *Structure characterization*

The crystal structures of different Sn-doped ZnO were analyzed by X-ray diffraction (XRD). As shown in Figure 3, all the samples could be indexed to wurtzite ZnO (JCPDS card No. 36-1451), and no other impurities were detected, except for the 9at% Sn-doped ZnO. When dopant reached 9at%, stannic oxide diffraction peaks appeared, the dopant migrate from ordered substitutional sites within the lattice to more disordered regions, resulting in the shift of peaks toward lower 2θ value compared with other Sn-doped ZnO. The result also shows that 7at% doping is an optimal doping content without other impurity peaks.

The crystal structure of Sn-doped ZnO annealed at different temperatures was analyzed by XRD. As seen in Figure 4, all the samples have a similar wurtzite phase, and no other impurities were detected when the annealing temperature was less than 600°C. When the annealing temperature reached 700°C, the XRD results show some weak stannic oxide diffraction peaks. With the increase of annealing temperature (300-600°C), the intensity of diffraction peaks increased and the crystallinity improved, which indicated that higher annealing temperature was helpful to crystallize of Sn-doped ZnO materials. The results also show that there has an optimal annealing temperature.

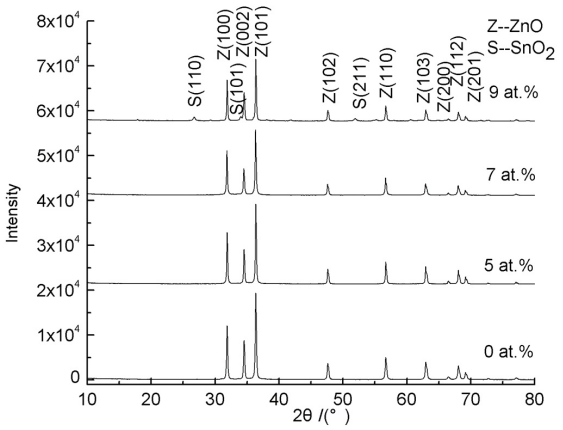

Figure 3. X-ray diffraction of different Sn-doped ZnO annealed at 600 °C for 1h.

Compared with Figure 3 and Figure 4, both the doping amounts and annealing temperature were important to the crystal structures, after more than a certain degree, impurity peaks appeared, and ZnO materials appears supersaturated.

The mean crystallite size (D) of the undoped and Sn-doped ZnO films can be deduced from the XRD peaks using the Scherrer's formula:

$$D = \frac{0.89\lambda}{\beta \cos\theta} \quad (1)$$

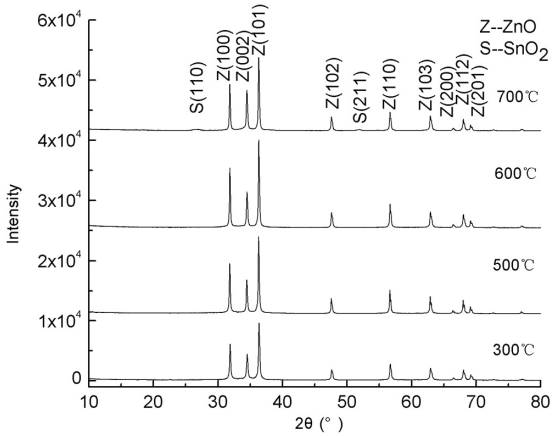

Figure 4. X-ray diffraction of 7 at% Sn-doped ZnO annealed at different temperatures for 1h.

Where λ is the X-ray wavelength, β is the full width at half maximum intensity (FWHM) and θ is the Bragg's angle of the XRD peak. The mean crystallite size is about 50nm.

The difference in the annealing temperature of Sn-doped ZnO materials is a key factor that has an important effect on the sensing performance. The morphologies of the samples were examined by SEM. As can be seen from Figure 5, both of them were six-prismatic structure. With the increase of annealing temperature, the experimental results show that the crystallinity has improved and the grain size has increased. In Figure 5 (600°C), the Sn-doped ZnO appeared rough porous structures and proper grain size, which was propitious to the gas's adsorption.

3.2. *Gas sensing performance*

3.2.1. Sensitivity of different samples for various gases

The sensitivity of different doping for various gases is shown in Figure 6. The samples of C0, C5, C7 and C9 were chosen for the test. (Testing conditions: operating temperature at 65°C, 1000ppm, under visible light,30%RH). It can be seen obviously that the sensitivities to methanol, ammonia, and toluene were much lower than that of ethanol. Especially, the 7 at% doped ZnO showed the highest sensitivity to ethanol. The results implied that the Sn-doped ZnO had a good selectivity to ethanol at appropriate condition. The reason would be interpreted later.

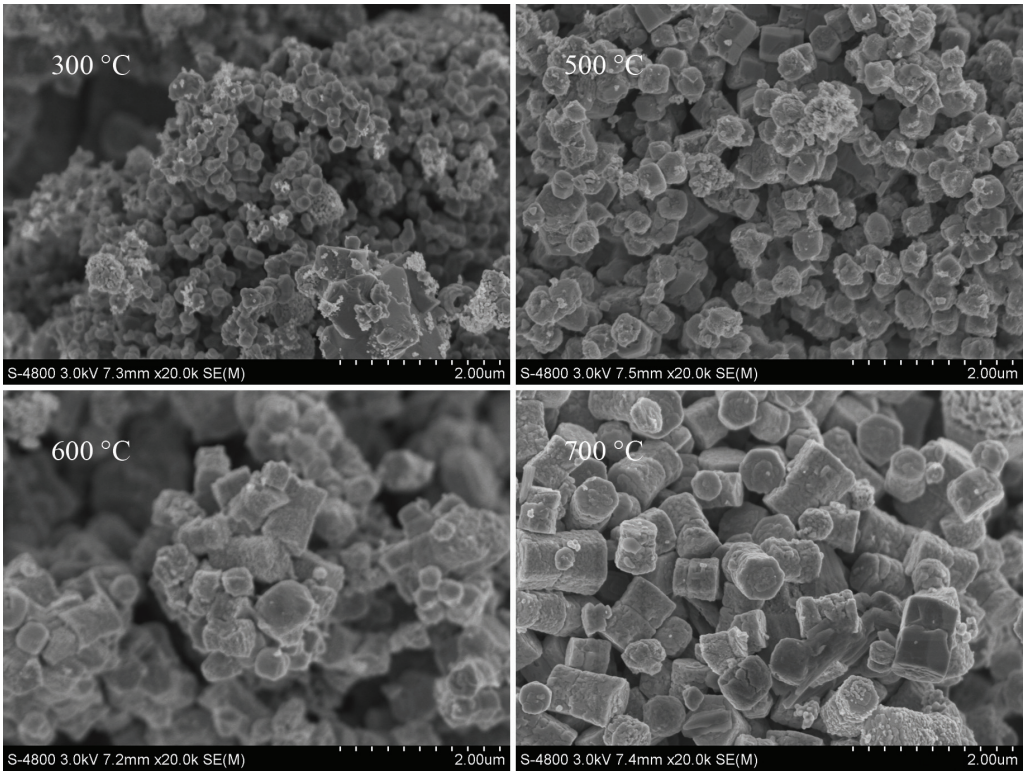

Figure 5. SEM images of 7 at% Sn-doped ZnO annealed at different temperatures.

3.2.2. The effect of visible light for pure ZnO gas sensors

Figure 7 shows the voltage response of ZnO under the visible light irradiation and ZnO in dark to 1000 ppm ethanol with operating temperature at 65°C in air-ambient of 30% RH. Both sensors responded immediately when the ethanol gas was introduced in the test chamber. There were similar response curve of sensors A and B. This is because ZnO is a wide bandgap (~3.4eV) material[2], the energy of visible light could not activate the electron of valence band. Thereby, we concluded that the visible light has no influence on pure ZnO gas sensors.

As seen in Figure 7, the response and recovery had little difference of curve A and B, taking ~8s and ~15s for 90% of full response and recovery, respectively. We also observed that the Vout could not return to the initial value after ethanol gas were discharged, this is because a few ethanol molecules were not likely to desorb thoroughly from the sensor surface, and we will also discussed further in the context.

3.2.3. The effect of visible light for Sn-doped ZnO gas sensors

The effect of visible light for Sn-doped ZnO gas sensors were tested using gas sensing test system. Figure 8 shows the dynamic response of 7 at% Sn-doped ZnO under the visible light irradiation (C) and 7 at% Sn-doped ZnO in dark (D) to 1000 ppm ethanol with operating temperature at 65°C in air-ambient of 30% RH. It is found that the voltage (Vout) of the load resistor which reflected the sensors' resistivity respond rapidly as ethanol gas was injected into the chamber and then purged. As can been seen from Figure 8, the response and recovery times of sensor C were ~1s and ~5s, respectively. However, the times of sensor D were ~4s and ~8s, respectively. Compared with pure ZnO sensors, the 7 at% Sn-doped ZnO sensors had a fast response and recovery time. B. L. Zhu et al. also researched the gas sensor of thick film ZnO, however, the response and recovery time was around 10 and 5 s, respectively, at operating temperature>320°C[15]. We also observed that the initial output voltage (Vout) of sensor C was higher than sensor D, which indicated that the resistance of C is lower than D. As is known to us all, Sn atoms can rearrange themselves into more suitable positions during the annealing process, which had been identified by the XRD spectra, and generate a new dopant energy below the conduction band of ZnO[11]. Thus, less energy is required by an electron to jump into the conduction band. When the Sn-doped ZnO was illuminated by the visible light, the photo-generated electrons would be excited to the conducting band of ZnO, resulting in the decrease of sensor's resistance. The result showed that visible light irritation had an obvious effect. However, this result had never been reported before through experimental verification.

3.2.4. Sensitivity comparison of different samples

Figure 9 showed the sensitivity (S) of pure ZnO in dark (1), pure ZnO under visible light (2), 7at% Sn-doped ZnO in dark (3), and 7at% Sn-doped ZnO under visible light(4), respectively. All of the four sensors were tested in the identical experimental conditions (At 1000ppm ethanol, operating temperature 65°C, 30% RH). As can been seen, column 1 and 2 had almost the same low sensitivity whereas under the visible light or not. The results were in accordance with Figure 7. By comparison, 7 at% Sn-doped ZnO (column 3 and 4) exhibited significantly high sensitivity, especially the column 4, achieved of 400. The high sensitivity may

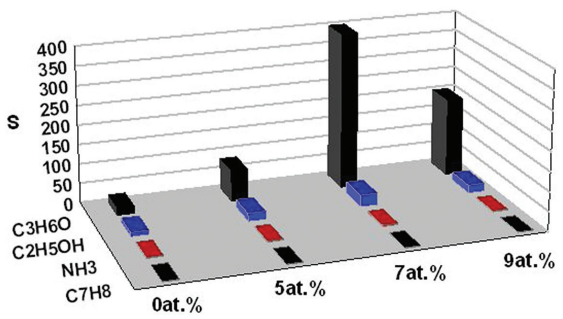

Figure 6. Sensitivity of different doping for various gases.

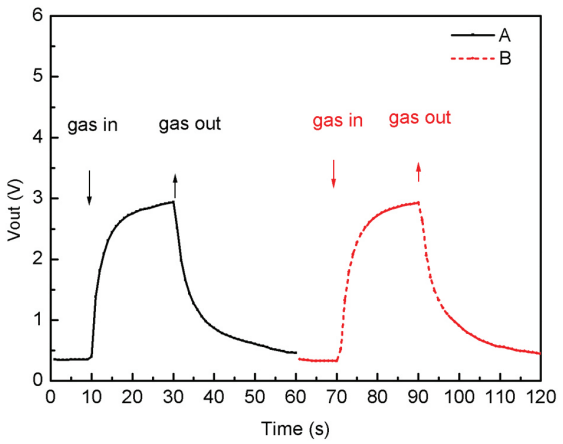

Figure 7. Curve A—pure ZnO under the visible light irradiation, Curve B—pure ZnO in dark.

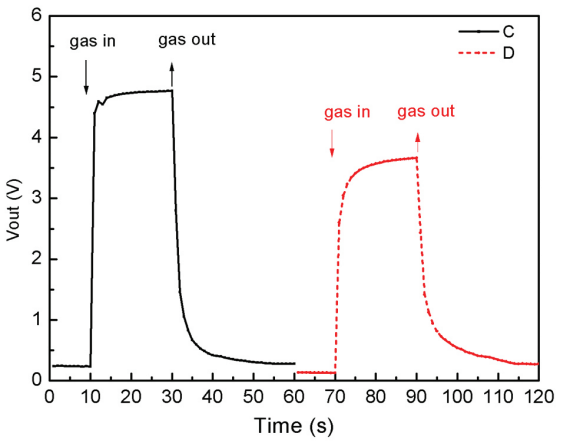

Figure 8. Curve C—7 at% Sn-doped ZnO under the visible light irradiation, Curve D—7 at% Sn-doped ZnO in dark.

be attributed to the individual mechanism which we will discuss later.

3.3. *Sensing mechanism*

It is well known that the sensing mechanism of ZnO-based sensors belongs to the surface-controlled type, that is, the resistance change is controlled by the species and amount of chemisorbed oxygen on surface[15]. The ethanol-sensing mechanism of the pure ZnO film may be explained as follows. Initially the molecular Oxygens were adsorbed on the surface of ZnO film and electrons were consumed following the reactions[16,17]:

$$O_2(gas) \leftrightarrow O_2(adsorbed) \tag{2}$$

$$O_2(adsorbed) + e^- \leftrightarrow O_2^-(adsorbed) \tag{3}$$

$$O_2^-(adsorbed) + e^- \leftrightarrow 2O^-(adsorbed) \tag{4}$$

thus increase of the film resistance.

When the ZnO film sensor was exposed to the ethanol, its atoms reacted with these chemisorbed oxygen ions and produced CO_2 and H_2O molecules consuming chemisorbed oxygen from the surface by releasing electrons. The reaction can be represented by the following relation:

$$C_2H_5OH + 6O^-(adsorbed) \rightarrow 2CO_2 + 3H_2O + 6e^- \tag{5}$$

As a result electrons were released back to the conduction band, thereby decreasing the resistance of the film. The reaction was exothermic in nature which was helpful to desorption.

However, under visible light irradiation, compared with pure ZnO, the Sn-doped ZnO showed a big difference. A close correlation was found between Sn-doped ZnO under visible light irradiation and gas sensitivity based on which an appropriate mechanism underlying this phenomenon was suggested.

Firstly, we discussed the 7 at% Sn-doped ZnO in dark condition, the sensitivity of Sn-doped ZnO film was higher than that of pure ZnO, which can be ascribed to the more active adsorption centers produced by the dopant. In addition, the amount of adsorption of O^{2-} and O^- species had been shown to be fairly small (less than 1% in surface coverage), suggesting that their adsorption is limited by the supply of electrons[18]. However, Sn^{4+} can act as donors of conduction electrons and thus adsorbed more oxygen[19]. Therefore, the sensitivity of Sn-doped ZnO was better than pure ZnO samples.

When 7 at% Sn-doped ZnO were tested under the visible light irradiation, the sensitivity had a sharp increasing immediately. Through this phenomenon, our group put forward a hypothesis for further explanations. As reported before, Sn-doping can generate some new doping levels below the conduction band of ZnO[11]. When visible light radiation fell on the Sn-doped ZnO polycrystalline film, photoactivated electrons were generated in the conduction band. Optical excitation decreased the inter-grain barrier height, thereby increasing the density of free carriers through the material[20]. As a result, the ambient oxygen molecules reacted with the photoelectrons as follows[21,22]:

$$h\nu \rightarrow h^+ + e^- \tag{6}$$

$$O_2 + e^-(h\nu) \rightarrow O_2^-(h\nu) \tag{7}$$

Upon exposure to C_2H_5OH, the photoinduced oxygen ions $\left(O_2^-(h\nu)\right)$ that participate in the redox reaction.

$$C_2H_5OH + 3O_2^-(h\nu) \rightarrow 2CO_2 + 3H_2O + 3e^- \tag{8}$$

The electrons released from this process result in the decrease of resistance of ZnO film. These photoinduced oxygen ions $\left(O_2^-(h\nu)\right)$ were highly reactive and responsible for the gas sensitivity.

Activation energy is an important basis for the study of gas sensing-mechanism, and is helpful to provide a gas-sensing material with good performance. Therefore, we calculated the activation energy, using the following formula[23]:

$$R = Ce^{E/kT} \tag{9}$$

Where C is a constant, E is the activation energy, associated with the formation of lattice defects, k is the Boltzmann's constant, and R is the sample resistance.

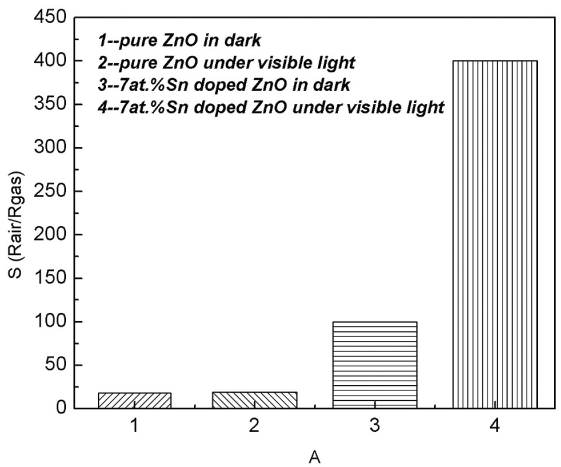

Figure 9. Sensitivity of different samples.

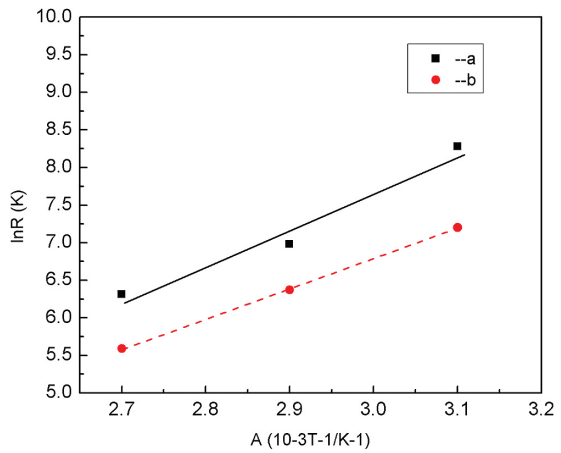

Figure 10. lnR-1/T curve.

We measured the resistance of pure ZnO samples and 7at% Sn-doped ZnO samples at different temperature 45°C, 65°C and 85°C, and made the lnR-1/T curve, as shown in Figure 10, a is the curve of pure ZnO samples, b is the curve of Sn-doped ZnO samples.

From Figure 10, the activation energy of curve a (Ea) is 0.60eV, and the Eb is 0.39eV. The Sn-doping generates a lot of defect levels among bandgap, reduces the reaction activation energy, and changes the resistance. The activation energy lowered 0.21eV. The low activation energy of Eb is contributed to improve the gas sensing characteristics.

4. Conclusion

We prepared a thick film ethanol gas sensor by the chemical co-precipitation method and characterized the samples by X-ray diffraction and scanning electron microscopy, respectively. The characterization results showed that all the samples were wurtzite with hexagonal structure and were well crystallized. Under the visible light irradiation, the 7 at% Sn-doped ZnO showed short response time and high selectivity towards ethanol vapor. The operating temperature was 65°C and the response and recovery time were ~1s and ~5s, respectively, which were very important for commercial application. The activation energy was 0.39eV. We also discussed the sensitive mechanism of gas-sensitivity and photo-sensitivity synergistic effect.

Acknowledgements

This work was supported by the Major National Science and Technology Special Projects, China (No. 2009ZX02308-004) and the National Natural Science Foundation of China (No. 60972106). The authors are also grateful to the Analysis and Testing Center of Hebei University of Technology.

References

1. Barsan N, Koziej D and Weimar U. Metal oxide-based gas sensor research: how to? *Sensors and Actuators B*. 2007; 121(1):18-35. http://dx.doi.org/10.1016/j.snb.2006.09.047
2. Schmidt-Mende L and MacManus-Driscoll JL. ZnO: nanostructures, defects, and devices. *Materials Today*. 2007; 10(5):40-48. http://dx.doi.org/10.1016/S1369-7021(07)70078-0
3. Korotcenkov G. Gas response control through structural and chemical modification of metal oxide films: state of the art and approaches. *Sensors and Actuators B: Chemical*. 2005; 107(1):209-232. http://dx.doi.org/10.1016/j.snb.2004.10.006
4. Han N, Wu XF, Zhang DW, Shen GL, Liu HD and Chen YF. CdO activated Sn-doped ZnO for highly sensitive, selective and stable formaldehyde sensor. *Sensors and Actuators B: Chemical*. 2011; 152(2):324-329. http://dx.doi.org/10.1016/j.snb.2010.12.029
5. Cheng XL, Zhao H, Huo LH, Gao S and Zhao JG. ZnO nanoparticulate thin film: preparation, characterization and gas-sensing property. *Sensors and Actuators B: Chemical*. 2004; 102(2):248-252. http://dx.doi.org/10.1016/j.snb.2004.04.080
6. Arshak K and Gaidan I. Development of a novel gas sensor based on oxide thick films. *Materials Science and Engineering B*. 2005; 118(1):44-49. http://dx.doi.org/10.1016/j.mseb.2004.12.061
7. Neri G, Bonavita A, Rizzo G, Galvagno S, Capone S and Siciliano P. Methanol gas-sensing properties of CeO2-Fe2O3 thin films. *Sensors and Actuators B: Chemical*. 2006; 114(2):687-695. http://dx.doi.org/10.1016/j.snb.2005.06.062
8. Sun JB, Xu J, Yu YS, Sun P, Liu FM and Lu GY. UV-activated room temperature metal oxide based gas sensor attached with reflector. *Sensors and Actuators B: Chemical*. 2012; 169:291-296. http://dx.doi.org/10.1016/j.snb.2012.04.083
9. Chu XF, Jiang DL, Djurišic AB and Leung YH. Gas-sensing properties of thick film based on ZnO nano-tetrapods. *Chemical Physics Letters*. 2005; 401(4-6):426-429. http://dx.doi.org/10.1016/j.cplett.2004.11.091
10. Caglar Y, Aksoy S, Ilican S and Caglar M. Crystalline structure and morphological properties of undoped and Sn doped ZnO thin films. *Superlattices and Microstructures*. 2009; 46(3):469-475. http://dx.doi.org/10.1016/j.spmi.2009.05.005
11. Han L, Wang D, Lu Y, Jiang T, Chen L, Xie T et al. Influence of annealing temperature on the photoelectric gas sensing of Fe-doped ZnO under visible light irradiation. *Sensors and Actuators B: Chemical*. 2013; 177:34-40. http://dx.doi.org/10.1016/j.snb.2012.10.096
12. Fun ZX, Sun YC and Chen JL. Semiconductor transparent conductive films. *Chinese Journal of Semiconductors*. 2001; 22:589-592.
13. Xu JQ, Han JJ, Zhang Y, Sun YA and Xie B. Studies on alcohol sensing mechanism of ZnO based gas sensors. *Sensors and Actuators B: Chemical*. 2008; 132(1):334-339. http://dx.doi.org/10.1016/j.snb.2008.01.062
14. Yang ZX, Huang Y, Chen GN, Guo ZP, Cheng SY and Huang SZ. Ethanol gas sensor based on Al-doped ZnO nanomaterial with many gas diffusing channels. *Sensors and Actuators B: Chemical*. 2009; 140(2):549-556. http://dx.doi.org/10.1016/j.snb.2009.04.052
15. Zhu BL, Xie CS, Wang WY, Huang KJ and Hu JH. Improvement in gas sensitivity of ZnO thick film to volatile organic compounds (VOCs) by adding TiO2. *Materials Letters*. 2004; 58(5):624-629. http://dx.doi.org/10.1016/S0167-577X(03)00582-2
16. Sahay PP and Nath RK. Al-doped ZnO thin films as methanol sensors. *Sensors and Actuators B: Chemical*. 2008; 134(2):654-659. http://dx.doi.org/10.1016/j.snb.2008.06.006
17. Lupan O, Chai G and Chow L. Novel hydrogen gas sensor based on single ZnO nanorod. *Microelectronic Engineering*. 2008; 85(11):2220-2225. http://dx.doi.org/10.1016/j.mee.2008.06.021
18. Yamazoe N and Shimanoe K. Receptor function and response of semiconductor gas sensor. *Journal of Sensors*. 2009; 2009:1-21. http://dx.doi.org/10.1155/2009/875704
19. Yamazoe N, Sakai G and Shimanoe K. Oxide semiconductor gas sensors. *Catalysis Surveys*. 2003; 7(1):63-65. http://dx.doi.org/10.1023/A:1023436725457
20. Mishra S, Ghanshyam C, Ram N, Bajpai RP and Bedi RK. Detection mechanism of metal oxide gas sensor under UV radiation. *Sensors and Actuators B: Chemical*. 2004; 97(2-3):387-390. http://dx.doi.org/10.1016/j.snb.2003.09.017
21. Zhai JL, Wang LL, Wang DJ, Lin YH, He DQ and Xie TF. UV-illumination room-temperature gas sensing activity of carbon-doped ZnO microspheres. *Sensors and Actuators B: Chemical*. 2012; 161(1):292-297. http://dx.doi.org/10.1016/j.snb.2011.10.034
22. Fan SW, Srivastava AK and Dravid VP. UV-activated room-temperature gas sensing mechanism of polycrystalline ZnO. *Applied Physics Letters*. 2009; 95(14):142106-142108. http://dx.doi.org/10.1063/1.3243458
23. Zhou W, Sun CW and Yang ZZ. Research and development of titania oxygen sensors. *Journal of Inorganic Materials*. 1998; 13(3):275-281.